Efficient cascaded parameter scan approach for studying top-off safety in storage rings

Yongjun Li, Lingyun Yang, and Samuel Krinsky
Brookhaven National Laboratory, Upton, New York 11973, USA
(Received 22 November 2010; published 8 March 2011)

We introduce a new algorithm, which we call the cascaded parameter scan method, to efficiently carry out the scan over magnet parameters in the safety analysis for top-off injection in synchrotron radiation storage rings. In top-off safety analysis, one must track particles populating phase space through a beam line containing magnets and apertures and clearly demonstrate that, for all possible magnet settings and errors, all particles are lost on scrapers within the properly shielded region. In the usual approach, if one considers m magnets and scans each magnet through n setpoints, then one must carry out n^m tracking runs. In the cascaded parameter scan method, the number of tracking runs is reduced to $n \times m$. This reduction of exponential to linear dependence on the number of setpoints n greatly reduces the required computation time and allows one to more densely populate phase space and to increase the number n of setpoints scanned for each magnet.

DOI: 10.1103/PhysRevSTAB.14.033501 PACS numbers: 29.20.dk, 29.27.Ac

I. INTRODUCTION

Many third-generation synchrotron light sources are running with top-off injection, which was first adopted by the Advanced Photon Source at Argonne National Laboratory [1]. In this operation mode, the stored beam current is maintained at quasiconstant level through frequent injection. In the National Synchrotron Light Source II (NSLS-II) [2], a 3 GeV high-brightness synchrotron radiation source which is under construction at Brookhaven National Laboratory, we plan to provide a 500 mA beam current with 1% intensity stability for users by employing top-off injection once per minute. An important safety issue is raised here: during injection with user beam line safety shutters open, injected beam must not be allowed to escape past all physical apertures and pass beyond the shield wall. One must assure that fault conditions, e.g., due to the shorts of dipole magnets, or mismatch of injected beam energy etc., cannot lead to an unsafe condition.

To assure the safety in top-off injection mode, detailed simulation studies have been performed for existing and under-construction machines [3–9]. In top-off safety analysis, a complete parameter scan must cover: (1) the possible permutations of magnet settings and errors (settings mean magnets are at different excitations, and errors represent magnets have some faults); (2) the particles populating the area in phase space restricted by physical apertures; (3) the range of beam energy deviation due to the mismatch between injection system and storage ring. Based on the simulation results, both sufficient fixed apertures (passive protection) and hardware interlocks (active protection) need to be specified to prevent injected beam from escaping through the open beam line safety shutters despite possible machine equipment faults. Therefore an efficient and conservative algorithm to scan parameters is needed for top-off safety simulation.

This paper presents a new method, which we call cascaded parameter scan, for analyzing fault conditions. In Sec. II, the usual method to scan parameters is discussed. The cascaded parameter scan approach is introduced in Sec. III. In Sec. IV we discuss a key aspect of the new approach, repopulation in phase space, which plays an important role in dramatically shortening computation time. The process of retracing unsafe particles, identifying unsafe machine scenarios and particle trajectories, is presented in Sec. V. An example of applying the cascaded parameter scan method to study one of the NSLS-II beam lines is given in Sec. VI. In Appendix A, we discuss how to include energy scan by correspondingly extending magnet scan ranges.

II. TREE-SHAPED PARAMETER SCAN AND ITS DIFFICULTIES

To assure safety, the parameter scan for top-off safety tracking needs to be complete and conservative, covering all the possible permutations of magnet settings and errors. For example, if there exist totally k magnets (Fig. 1) in a beam line from its radiation source point to the front-end safety shutter, and for each magnet ($i = 1, 2, \ldots, k$) we use n_i discrete setpoints to cover its continuous full-range excitations and errors, the number of magnet fault permutations is $\prod_{i=1}^{k} n_i$. A straightforward method is to perform the parameter scan over the tree-shaped structure as shown in Fig. 2. Typically there are about 10 to 12 magnets which must be taken into account in analyzing a NSLS-II insertion device beam line. If each magnet is chosen with ten steps to represent its possible settings and errors, then the

Published by American Physical Society under the terms of the Creative Commons Attribution 3.0 License. Further distribution of this work must maintain attribution to the author(s) and the published article's title, journal citation, and DOI.

 © 2011 American Physical Society

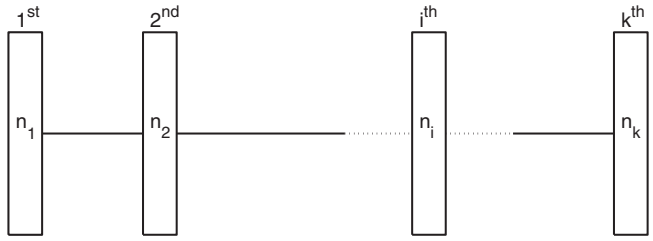

FIG. 1. Layout of a beam line with k magnets, each of which has $n_i (i = 1, 2, \ldots, k)$ setpoints to represent its different excitations and shorts.

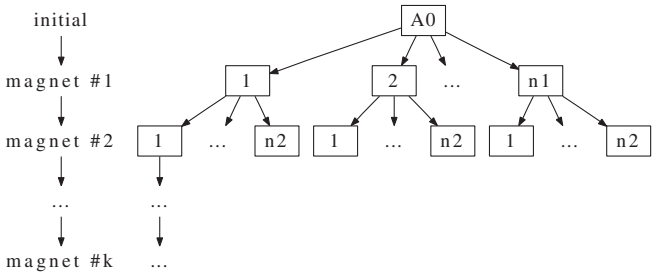

FIG. 2. Diagram of permutations in the tree-shaped parameter scan. A_0 is the initial conditions in phase space. It evolves into n_1 areas after the first magnet with n_1 setpoints, and then $n_1 \times n_2$ after the second magnet, and so on. The number of permutations increases exponentially with the number of magnet setpoints.

total number of permutations is 10^{10}–10^{12}. Although some branches in the tree may not need to be scanned because no particle can survive from their parent branches, still a huge number of permutations remain.

Although we only need to track particles through a limited number of magnets to analyze a beam line's top-off safety, it is still a very time-consuming computation process even with parallel computation. To be complete and conservative, if it is found to be necessary to increase the number of considered setpoints of magnet settings and errors, the number of permutations increases exponentially, and the whole scan process becomes very complex. To overcome these difficulties, we propose a new and more efficient approach, cascaded parameter scan, which can shorten the computation time dramatically without loss of completeness.

III. CASCADED PARAMETER SCAN

In this and the next sections, we explain the process of cascaded parameter scan and repopulation, and discuss why it is more efficient than the usual method. Consider the same beam line as in the previous section. After tracking initial particles to arrive at the first magnet entrance, we get a closed phase space area A_1^- composed of an assembly of phase space points (see Fig. 3). The first magnet is assumed to have n_1 setpoints covering all the possible errors and excitations. We then track A_1^- through the

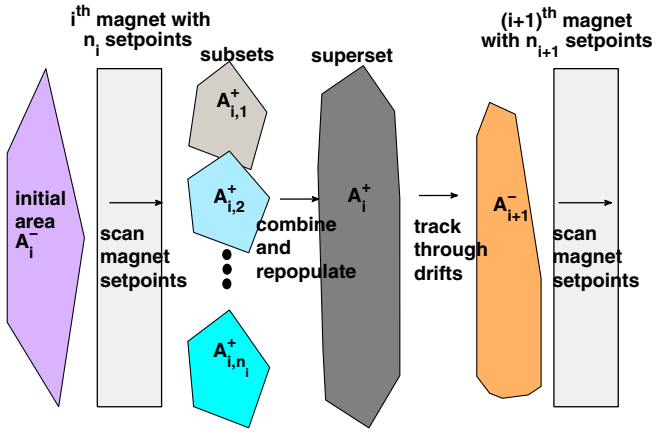

FIG. 3. Combination of subsets into a superset. We scan all the ith magnet setpoints separately for the same initial input A_i^-, then combine them into a superset A_i^+. Next we track A_i^+ to the entrance of the next magnet to get A_{i+1}^-, and then repeat the same process.

magnet for each of its n_1 setpoints, and obtain n_1 closed areas $A_{1,i}^+ (i = 1, 2, \ldots, n_1)$ at the magnet exit. We archive the coordinates x, x' of all of the particles in each subset $A_{1,1}^+, A_{1,2}^+, \ldots, A_{1,n_1}^+$ for the purpose of retracing (as explained in detail in Sec. V). Next we combine all the subsets into a superset A_1^+ using a repopulation technique in phase space (see Sec. IV). After obtaining the repopulated superset at the magnet exit, we use it as the input for subsequent tracking. The process of combining the subsets into a superset and repopulating it in phase space is repeated for the next magnets until the end of the beam line is reached, or all particles are stopped by the defined physical apertures. The process of obtaining the superset for the ith magnet is illustrated in Fig. 3.

During tracking, if particle amplitudes exceed beam line physical apertures, they will be removed from the data pool and considered as safe. If there is no particle surviving through all the physical apertures, the beam line is safe. But if there are some particles going through all physical apertures, this beam line is potentially unsafe. We need to retrace these unsafe particles back into the magnet subsets in the opposite sequence of the cascade parameter scan to find out the corresponding magnet settings. Interlocks can then be designed to restrict magnet ranges to avoid unsafe conditions. The detailed retracing process will be addressed in Sec. V.

IV. REPOPULATION OF PARTICLES IN PHASE SPACE

In the cascaded parameter scan, if we simply combine all the particles in subsets into a superset, the number of particles will increase exponentially with the number of magnet setpoints, and the amount of computation scales the same as for the usual tree-shaped scan. For a given initial

area in phase space at the magnet entrance, the corresponding subsets for different excitations or errors at the magnet exit will usually have some overlaps, because we use discrete setpoints to approximate a continuously variable magnetic field. It is easy to see that, in the overlapped region, the density of particles becomes very high after many overlaps, and the distance in phase space between some particles becomes very small. These overdensely distributed particles represent conditions which are very close in phase space. Since we are studying a symplectic system, the area in phase space evolving under magnetic field is continuous and conserved. Therefore, overdense points will not provide more useful information, but just waste computation time. In a word, the purpose of adopting a repopulation technique is to avoid redundant tracking.

The implementation of repopulation is as follows: First, we combine all subsets at the magnet exit into a superset and define an area (usually it is a rectangle, see the largest rectangle in dash line in Fig. 4) which can cover all the points in the superset. Then, we divide this area with a sufficiently small mesh grid. Next, all the particles in the superset are projected onto this mesh grid according this rule: if there are any particles located within a grid (including on its borders), we will use the four points at the surrounding grid vertices to represent them. In the overlapping region of subsets, although the density inside a small rectangle can be very high, after repopulation four particles at the grid corners will adequately represent them. The schematic process of the repopulation technique is shown in Fig. 4. After the repopulation, the number of

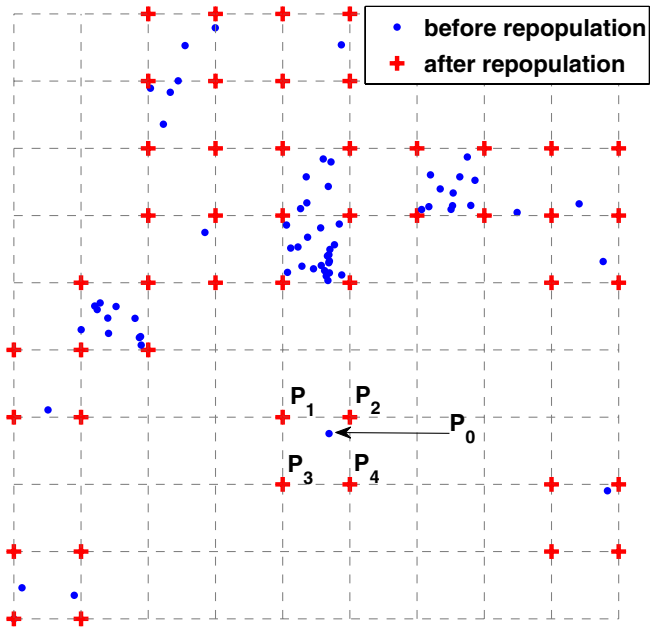

FIG. 4. Illustration of repopulation technique in phase space. Blue points are original points in the superset, which may have high density in reality; red crosses are the points after repopulation; gray dashed lines show the mesh grid.

populated particles is proportional to the actual occupied area in phase space instead of the number of the magnet setpoints. In this way, we reduce the dependence of the number of tracking runs on the number of magnet setpoints from exponential to linear.

Special care has to be taken when applying the repopulation technique, because some unphysical particles have been introduced into the superset at its borders. For example, consider the original particle P_0 located within a grid and its four vertices P_1, P_2, P_3, and P_4 (see Fig. 4). After repopulation, the border of the original area is extended approximately by the order of the mesh grid dimension. Since we are studying a nonlinear dynamic system (the magnetic field profile is nonlinear), this area expansion could become quite large after passing through enough magnets. Thus, unphysical particles can be introduced into subsequent tracking by employing a series of repopulations. This method is not good for a long-term tracking, because the area in phase space will expand exponentially even for small grid dimensions. But in the top-off safety simulation, we only need to track particles through a small number of magnets. Once we choose the mesh grid fine enough, the area expansion in phase space is limited and controllable. In applying this method, we choose the suitable dimension of the mesh grid by decreasing it step by step until a convergent area is obtained after tracking through the whole beam line. Here convergence means the variation of boundaries are controlled under 0.2 mm and 0.1 mrad, which are much smaller than the whole area occupied by the potentially unsafe particles, and also the 2 mm tolerance on aperture position. In Fig. 5, two areas closed by red and blue lines, obtained by tracking the

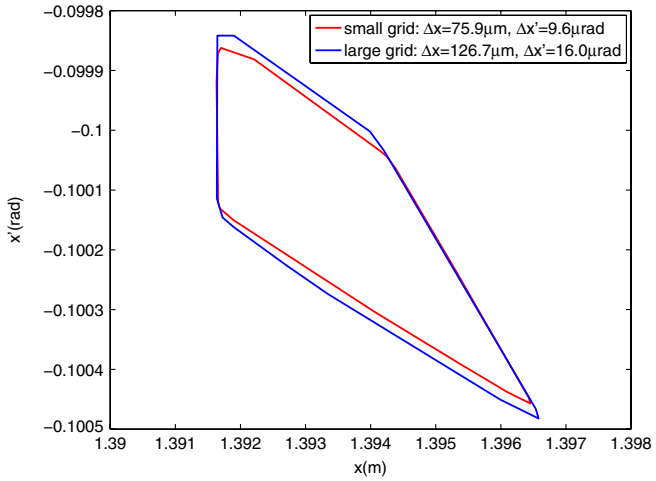

FIG. 5. Two areas are obtained by tracking the repopulated supersets with two different dimension mesh grids through the same beam line. The blue one is for the bigger dimension grid, and the red one for the smaller grid. With the decrease of mesh grid dimension step by step, two areas can be seen to be well overlapped (convergent), and then the further decrease of grid dimension becomes unnecessary.

repopulated supersets with two different dimension mesh grids, are seen to be well overlapped. Only in this case do we regard the mesh grid dimension is fine enough for the purpose of controlling the unphysical area expansion. Otherwise, it is necessary to further decrease the mesh grid dimension until convergence is reached.

V. RETRACING UNSAFE TRAJECTORIES

As we discussed in Sec. III, if some particles can pass through all the physical apertures in the cascaded parameter scan, this beam line is potentially unsafe. So in this section, we explain how we can identify the corresponding unsafe range of magnet settings and determine the unsafe particle trajectories by retracing the unsafe particles back into the initial conditions. Interlocks can then be employed to assure that magnet excitations are kept in a range for which there are no unsafe particles.

We use the ith magnet as an example to explain the process of retracing (see Fig. 6). We start from the coordinates of the unsafe particles in A_{i+1}^{-} at the entrance of the $(i+1)$th magnet, and retrace them into the superset A_i^{+} at the exit of the ith magnet. Then we check what particle coordinates lie within each unsafe mesh grid in A_i^{+}, and determine to which subset $A_{i,k}^{+}(k = 1, 2, \ldots, n_i)$ these particles belong. This tells us what values of the excitation (or what kinds of short) of the ith magnet can lead to unsafe particles. The coordinates x, x' of particles in subsets $A_{i,1}^{+}, \ldots, A_{i,n_i}^{+}$ corresponding to all magnet setpoints were archived for this purpose when we performed the cascaded parameter scan (see Sec. III). Next we track the unsafe particles back through the ith magnet at the corresponding excitations (or shorts) and find the unsafe particle coordinates in A_i^{-} at the entrance of the ith magnet. This procedure is iterated to take us from one end of the beam line to the other.

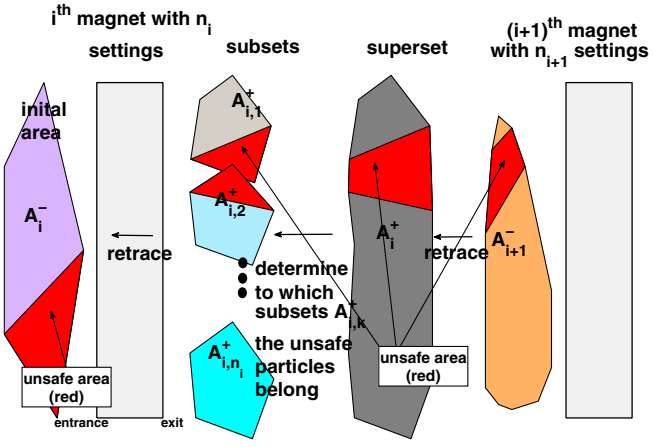

FIG. 6. Retracing unsafe phase space area to identify the unsafe magnet settings. The retracing is carried out in the opposite direction of the cascaded parameter scan. If the unsafe particles (area in red) at the ith magnet exit is found to belong to certain subsets ($A_{i,1}^{+}$ and $A_{i,2}^{+}$), it means unsafe particles can pass through this magnet under the corresponding setpoints (1st and 2nd). Next we retrace the unsafe area from the magnet exit to its entrance under the corresponding setpoints to obtain the unsafe area in A_i^{-}. We iterate this procedure from one end of the beam line to the other.

After retracing through the whole beam line, two important results can be obtained: First, we can determine the unsafe magnet setting ranges for which particles can pass through all the physical apertures. The unsafe magnet setting ranges can guide us to specify the necessary interlock requirements on magnet power supplies. Second, we can get the unsafe particle trajectories by connecting their coordinates between magnet entrances and exits. The trajectory information can be used to check the possibility to implement additional physical apertures to prevent them from passing through the beam line.

Thanks to the existence of physical apertures, in most cases, only part of the area of phase space at the entrance can pass through the exit apertures. Usually we perform two runs. In the first run, we do cascaded parameter scan, and then retracing to find potentially unsafe ranges. In the second run, we adopt sufficient interlocks or apertures, then redo parameter scan to confirm that no unsafe scenario can exist any longer. For the second run, the retracing process is not needed, because no particles can survive through all apertures once interlocks and apertures are sufficient.

VI. APPLICATION IN NSLS-II TOP-OFF SAFETY ANALYSIS

Here we use one of the NSLS-II baseline beam lines, x-ray powder diffraction (XPD) with its radiation source from a 7 m long damping wiggler, as an example to show how to apply our approach to detect unsafe scenarios and specify magnet power supply interlock requirements. The layout of the beam line is shown as Fig. 7. We want to prevent the injected beam from escaping through the photon shutter during the top-off injection.

We use the backward tracking approach [3,5], i.e., the cascaded parameter scan is performed by tracking particles from the photon shutter in the user beam line front-end back into the storage ring. The trajectory of an electron going from one point to another point in a pure magnetic field is the same as the trajectory of a positron moving in the opposite direction. Thus, if we can prove that no positron starting from the photon shutter in the front-end can enter the ring chamber acceptance with the existence of all physical apertures, we have proven that no electron starting from the ring acceptance can travel through the photon shutter under the same conditions.

One important assumption we adopted in our simulation is to perform the tracking study only in the midplane. In principle, we need to track particle trajectories in a 4D $x - x' - y - y'$ phase space. It turns out to be time consuming. So in order to simplify calculation, we only

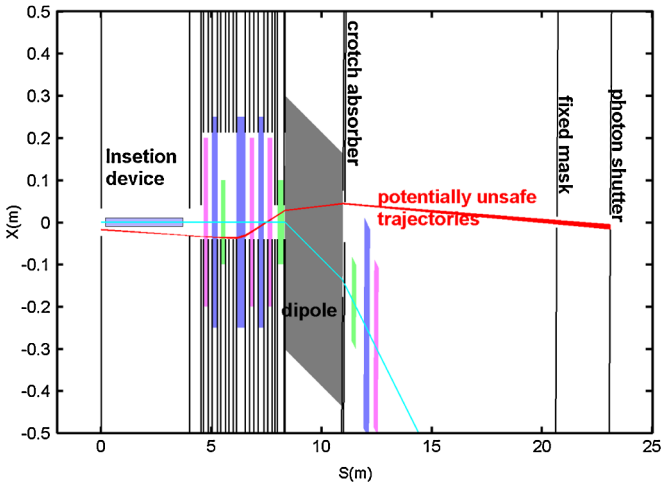

FIG. 7. The layout of XPD beam line with its source point from the damping wiggler at the long straight section. The cyan line is the stored beam orbit, which is used as a reference coordinate in tracking. The colored blocks centered along the stored beam orbit are magnets. The black lines with various openings represent the horizontal physical apertures restricted by machine vacuum enclosure and radiation collimators. The red lines are potentially unsafe trajectories under the magnet settings shown as Table I.

simulate particle motions in the midplane, but extend the scan range of quadrupole and sextupole field by an extra 7% to include the particle's vertical offsets [4].

Particle tracking also depends on the initial coordinates (positions and angles). Since there are no magnets in the beam line front end, it is easy to choose some physical apertures there to define the initial coordinates for tracking. In our simulation, we choose two physical apertures, the fixed mask and the photon shutter, to uniquely define a closed diamond area (Fig. 8) in phase space to contain all possible incident beam coordinates. Compared with the area occupied by the potentially unsafe particles, the diamond can be quite large. To assure the unsafe particles can be detected by parameter scan, the diamond must be uniformly populated with highly dense particles. Considering incident particles may have a certain range of energy deviation, the incident particle initial coordinates for tracking actually form a closed 3D volume in the phase space of $x - x' - \delta$. Here $\delta = \frac{E-E_0}{E_0}$ is particle energy deviation. We

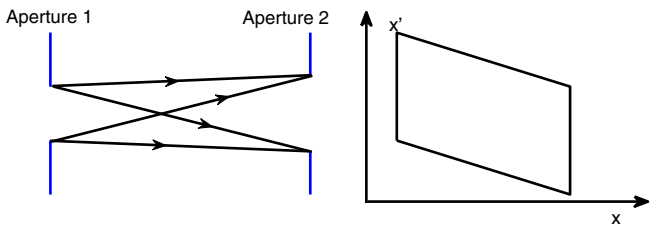

FIG. 8. Four rays determined by two physical apertures within a magnetic field free region uniquely define a diamond-shaped area in phase space at the initial tracking point.

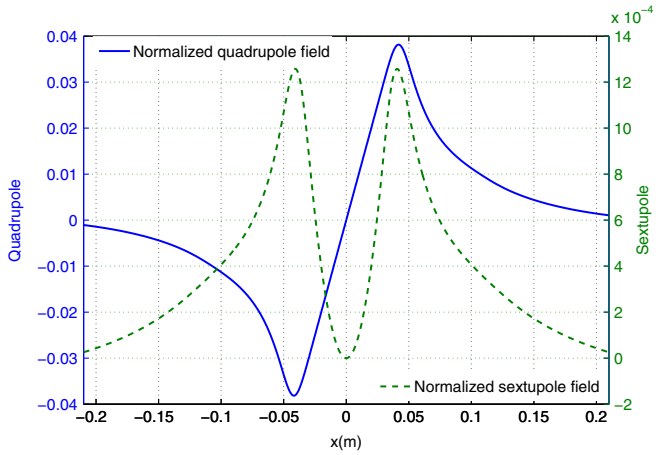

FIG. 9. Normalized transverse field profiles in the midplane for quadrupole (solid) and sextupole (dashed) without shorts. In the case of magnet shorts, the profiles do not have symmetry.

limit the range of energy deviation within $\delta = \pm 3\%$, and scan it with the fixed 1% step size. In Appendix A, we discuss an alternative method to scan energy by correspondingly extending magnet scan ranges.

The magnetic field data to describe all magnet settings and errors have been calculated with the code OPERA [10] in advance. Within the allowed range of power supply capacities, the magnetic fields are proportional to their excitation currents, and the profiles are approximately unchanged [11]. We calculate the magnetic field maps at a certain excitation, then normalize them with the corresponding gradient value to get the profiles. Figure 9 shows the profiles of quadrupole and sextupole without shorts. The field profiles should be wide enough in the midplane to cover the vacuum chamber dimension, because mis-steering injected beam can result in very large horizontal amplitudes. As seen in Fig. 9, the quadrupole (sextupole) field is far from linear (quadratic) and turns over as one gets beyond the poles of the magnet. Therefore the fast symplectic integrator used in dynamic aperture simulation, like in [12], which assumes magnet field can be expressed in a simple polynomial form, does not always apply to top-off safety tracking. Some general but slow numerical integrators, e.g., classic Runge-Kutta integrator, accompanied by the numerical interpolations [13] have to be implemented to simulate particle trajectories. In order to obtain accurate particle trajectories, the step size of numerical integrations must also be small enough in the integration direction.

The initial cascaded parameter scan result shows there are some potentially unsafe trajectories for this beam line, if we let magnets vary within the ranges as shown in the second column of Table I. By retracing the unsafe particle trajectories back into the starting point, we identify the unsafe magnet setting ranges as shown in Table I. The unsafe particle trajectories are illustrated in Fig. 7 and their locations in phase space are illustrated in Fig. 10. The beam line is unsafe only when all the

TABLE I. Scan range and unsafe range for NSLS-II XPD beam line.

	Scan range		Unsafe range[e]					
			$\delta = -3\%$		$\delta = 0\%$		$\delta = 3\%$	
Magnet	ER[a]	ST[b]	ER	ST	ER	ST	ER	ST
SH1	0–1.07[c]	1–6	0–1.07	1–6	0–0.60	1–6		
QH1	0–1.07	1–4	0–0.10	2	0			
QH2	0–1.07	1–4	≥ 1.07		≥ 1.07			
SH3	0–1.07	1–6	0.50–1.07	3	0.80–1.07			
QH3	0–1.07	1–4	0–0.30	2	0–0.10		Safe	
SH4	0–1.07	1–6	0–1.07	1–6	0–1.07	1–6		
B1	0.87–1.03[d]		0.87–0.93		0.87–0.89			
SM1	0–1.07	1–6	0–1.07	1–6	0–1.07	1–6		
QM1	0–1.07	1–4	0–1.07	1–4	0–1.07	1–4		

[a]ER (excitation ratio) is defined as the ratio of setpoint to the maximum allowed excitation value.
[b]ST (short type) is the index of magnet errors. Here we assume both quadrupoles and sextupoles can have one partially (50%) or fully (100%) shorted pole. There are four short types for quadrupoles, and six short types for sextupoles [14].
[c]The scan ranges of quadrupole and sextupole are extended by an additional 7% to include particle vertical offsets.
[d]Dipole field scan range is chosen to be above 90% its nominal value, another $\pm 3\%$ comes from the maximum contribution of its back leg winding. NSLS-II dipoles are separated function dipoles. Therefore the field variations at different vertical offsets are negligible. For general cases, e.g., combined function dipoles, different field profiles may be needed for each different vertical offset.
[e]Here we only list the retracing results for three different energy deviations.

conditions in the ''unsafe range'' column in Table I hold simultaneously. This means, if we interlock any one of the magnets to avoid its unsafe range, the beam line will become safe. Since the dipole $B1$ is the most critical element and has a fixed field strength, we plan to interlock its total field to be above 98% of its nominal value, and also interlock the injected beam energy deviation to be less than $\pm 3\%$. This eliminates unsafe conditions. Detailed specifications on interlock requirements and aperture limitations will be implemented according to the actual hardware conditions.

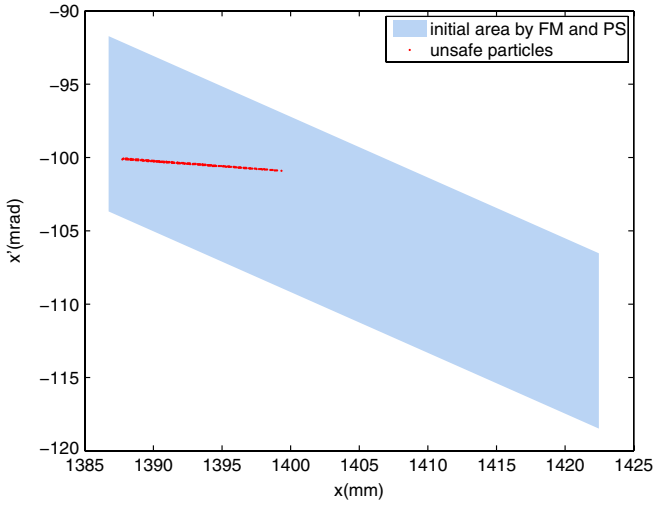

FIG. 10. The potentially unsafe particles (red points) location inside the initial diamond (light blue) defined by the fixed mask and the photon shutter. The unsafe particles only occupy a small area inside the diamond, so we need to populate enough particles inside the diamond in order to detect them. For this beam line, we use a mesh grid with the dimensions of 126 μm $\times$ 16 μrad. Therefore totally 160 000 particles are populated inside this diamond. We have tried some even smaller mesh grid, and got the same unsafe area. Interlocks are introduced to avoid unsafe parameter ranges.

VII. CONCLUSION

A new cascaded parameter scan algorithm, which can more efficiently carry out the parameter scan for top-off safety analysis, is proposed. This approach is illustrated by applying it to analyze a NSLS-II beam line. By converting the number of tracking runs from exponential to linear dependence on the number of magnet setpoints, the required computation time for a complete and conservative parameter scan is greatly reduced. This allows one to more densely populate phase space and to increase the number of setpoints scanned for each magnet.

ACKNOWLEDGMENTS

The authors would like to express their thanks to H. Nishimura and C. Steier from LBNL, and A. Terebilo and B. Hettel from SLAC for providing their simulation codes and sharing their experience at ALS and SSRL. We also thank B. Parker, M. Rehak, and C. Spataro for calculating magnet field profiles, and S. Sharma, H. Hsueh, L. Doom, and A. Hussain for providing the NSLS-II vacuum physical aperture information. This

work was supported by Department of Energy Contract No. DE-AC02-98CH10886.

APPENDIX A: SCAN OF PARTICLE ENERGY DEVIATIONS

As mentioned in Sec. I, the injected beam can have a certain range of energy deviation relative to the stored beam. In our simulation, we must scan over a range of particle energy deviations to define a safe window for the interlock requirements of the booster extraction system. A usual method to perform the energy scan is to use a few discrete values to represent the continuous range of injected beam energy deviation [5], and then perform a parameter scan for the fixed energy deviations independently.

It is possible to include the energy scan by increasing magnet scan ranges [6]. By observing the charged particle motion equation (A1) in a pure magnetic field,

$$\gamma_0 m_0 \frac{d\mathbf{v}}{dt} = q\mathbf{v} \times \frac{\mathbf{B}}{1+\delta}, \tag{A1}$$

where γ_0 is the Lorentz factor for the nominal energy particle $E_0 \approx cP_0$, m_0 the particle mass at rest, $\mathbf{v}$ the instantaneous velocity, t the time variable, q the charge, $\mathbf{B}$ the magnetic induction, $\delta = \frac{P-P_0}{P_0} \approx \frac{E-E_0}{E_0}$ the relative momentum deviation. Here the difference between energy and momentum deviation is negligible because of high particle energy. We note that the motion of an on-momentum particle is the same as an off-momentum particle with energy deviation δ moving in the same field profile but scaled by a factor $\frac{1}{1+\delta}$. Therefore we can include the energy scan into the magnet field scan by scaling the field variation range with this factor. For example, the full magnet excitation range is assumed as $[a, b]$, with $0 \leq a < b$, and we want to scan the energy deviation δ over $[-d, d]$, with $d > 0$. For particle with energy deviation $\delta = -d$, there exists an on-momentum particle, which will have the exact same trajectories within the magnet field scan range of $[\frac{a}{1-d}, \frac{b}{1-d}]$; and for energy deviation $\delta = d$, the corresponding range becomes $[\frac{a}{1+d}, \frac{b}{1+d}]$. That is, an off-momentum particle motion can be represented by an on-momentum particle with a scaled magnet scan range, which is energy dependent. In order to cover the energy deviation within $[-d, d]$, the union of all possible magnet scan ranges for an equivalent on-momentum particle is seen to be $[\frac{a}{1+d}, \frac{b}{1-d}]$.

The benefit of this approach is we can avoid some redundant calculation in the cascaded parameter scan. But a problem is also raised by extending the magnet scan ranges: some unphysical trajectories are introduced in the cascaded parameter scan. For example, a trajectory represents a particle passing through one magnet with an extended setpoint only for particles with positive energy deviation ($\delta > 0$), and then passes through another magnet with a setpoint only for particles with negative energy deviation ($\delta < 0$). Such trajectories are unphysical since the particle energy does not change during a single passing.

If the cascaded parameter scan shows that no particle can pass through all the physical apertures even after we extend the magnet scan range, the beam line will be safe, because all realistic cases are included after we extend the magnet scan range. If any trajectories are found to survive from all the physical apertures, we must exclude the unphysical trajectories from them. We found it is possible to eliminate the unphysical trajectories by considering the dependence of the magnet scan ranges on the particles energy in the retracing process. For the potentially unsafe trajectories obtained from the extended cascaded parameter scan to cover energy deviations range of $[-d, d]$, we retrace them back into the starting point with fixed energy deviation setpoints. Therefore we choose a series of setpoints $\delta = d_n$ $(n = 1, 2, \ldots)$ within the energy deviation $[-d, d]$. For each energy deviation setpoint d_n, the corresponding energy-dependent magnet scan ranges are $[\frac{a_i}{1+d_n}, \frac{b_i}{1+d_n}]$, $i = 1, 2, \ldots, k$ (in the cascaded parameter scan, the corresponding subsets for these magnet settings are calculated and archived). In retracing unsafe particles, we check whether the unsafe particles travel through each magnet within its allowed energy-dependent scan range. If not, then the particles are unphysical and are excluded. If any unsafe particles can be retraced to reach the starting point for a certain energy setpoint, then the beam line is unsafe for the particles with this particular energy deviation. Otherwise the beam line is safe for this energy deviation. After scanning over all the energy deviation setpoints $\delta = d_n$ $(n = 1, 2, \ldots)$, we will obtain the unsafe magnet ranges for each energy deviation. An interlock must be employed to assure that injected beam energy is kept in a range for which there are no unsafe particles.

[1] L. Emery and M. Borland, in Proceedings of the 18th Particle Accelerator Conference, New York, 1999 (IEEE, New York, 1999).
[2] "NSLS-II Preliminary Design Report" (2007), http://www.bnl.gov/nsls2/project/PDR/.
[3] M. Borland and L. Emery, in Proceedings of the 18th Particle Accelerator Conference, New York, 1999 (Ref. [1]).
[4] H. Nishimura *et al.*, in Proceedings of the 2007 Particle Accelerator Conference, Albuquerque, New Mexico (IEEE, Albuquerque, New Mexico, 2007).
[5] H. Nishimura *et al.*, Nucl. Instrum. Methods Phys. Res., Sect. A **608**, 2 (2009).
[6] A. Terebilo *et al.*, Report No. SSRL-ACC- PHYS NOTE-007, 2009.
[7] I. P. S. Martin *et al.*, in Proceedings of the 11th European Particle Accelerator Conference, Genoa, 2008 (EPS-AG, Genoa, Italy, 2008).
[8] Y. Asano and T. Takagi, Radiat. Meas. **41**, S236 (2006).

[9] Y. Li *et al.*, in Proceedings of the 23rd Particle Accelerator Conference, Vancouver, Canada, 2009 (IEEE, Piscataway, NJ, 2009).
[10] ''OPERA-2d&3d Reference Manual'', Vector Fields Inc., http://www.vectorfields.com/opera.php.
[11] A. Jain (private communication).
[12] H. Yoshida, Phys. Lett. A **150**, 262 (1990).
[13] ''MATLAB User Guide'' (2010), The MathWorks Inc., http://www.mathworks.com/.
[14] Y. Li *et al.* (unpublished).